

# Implementation and Fault Tolerance Benchmarking of the Fibonacci Quantum Error Correction Scheme for Near Term Quantum Computers

Jaebum Kim

August 2024

## Abstract

Near-term quantum processors offer a practical platform for evaluating fault-tolerant quantum computation; however, their performance remains constrained by physical error rates that exceed current fault-tolerance thresholds. Although quantum error correction (QEC) provides a theoretical mechanism for mitigating such errors, conventional codes typically incur significant resource overhead and circuit complexity, limiting their feasibility on near-term hardware. In this work, we present a classical simulation of Knill's Fibonacci quantum error correction scheme, implemented using the Qiskit framework. The scheme adopts a modular, Clifford-based architecture with recursive fault-tolerance properties, offering compatibility with contemporary quantum devices. Logical performance is assessed under depolarizing, bit-flip, and coherent noise models. The simulations demonstrate an approximate 50% reduction in logical error rates, largely invariant with respect to the underlying physical noise strength, indicating an intrinsic noise-agnostic suppression characteristic. Statistical reliability is maintained through a composite methodology that integrates rare-event sampling with Bayesian inference, enabling fine-grained resolution of logical error propagation. The complete implementation, including simulation data and code, is publicly available at: <https://github.com/EricKim1942/Fibonacci-Meets-Quantum-Computing>.

## I Introduction

### A. Quantum Computation and the Fibonacci Scheme

The implementation of fault-tolerant quantum computation remains impeded by persistent noise in gate operations, measurement processes, and qubit storage. While recent advances have extended coherence times and improved gate fidelities, physical error rates in current quantum devices continue to exceed the thresholds necessary for scalable quantum error correction (QEC). Leading QEC architectures, such as surface codes and concatenated stabilizer codes, provide strong asymptotic protection but incur considerable overhead in qubit count, connectivity, and circuit depth, limiting their applicability in noisy intermediate-scale quantum (NISQ) systems.

Fibonacci-style QEC, first introduced by Knill, presents an alternative approach based on recursive teleportation protocols and Clifford-group operations. This scheme employs a semi-recursive encoding hierarchy that confines fault propagation, supports transversal gate constructions, and reduces resource demands relative to uniformly concatenated codes. However, its performance under realistic noise models and limited recursion depth, conditions characteristic of near-term platforms, remains poorly understood.

In this study, we simulate the Fibonacci scheme using Qiskit's stabilizer formalism, focusing on Level-1 and Level-2 recursion tailored to contemporary hardware constraints. Logical error rates are evaluated across Pauli, depolarizing, and mixed coherent noise models. To ensure statistical rigor, we integrate multi-level splitting, cross-entropy adaptive sampling, large-deviation analysis, and Bayesian inference, enabling fine-grained estimation of logical error

suppression.

Our results reveal a consistent 50% reduction in logical error rates across all noise regimes, with suppression relatively insensitive to the specific physical error model. These findings highlight the practical viability of teleportation-based, recursive QEC for near-term devices and motivate further exploration of non-lattice fault-tolerance architectures with reduced resource overhead.

### B. Technical Gap in the Literature

Topological codes, especially the surface code, are widely regarded as foundational to fault-tolerant quantum computation due to their high noise thresholds and compatibility with local interactions. Nonetheless, their implementation demands substantial physical resources, including large qubit arrays, frequent stabilizer measurements, and rigid lattice connectivity requirements that exceed the capabilities of current hardware with constrained qubit counts and sparse coupling graphs. Concatenated codes, such as Steane and Bacon-Shor, offer modularity and support for transversal operations but suffer from rapidly increasing overhead with recursion depth, rendering them impractical for near-term architectures.

Fibonacci-style error correction presents an alternative paradigm that combines recursive encoding with teleportation-based fault isolation. By enabling selective rather than uniform recursion, these schemes reduce circuit depth and ancilla requirements while preserving fault-tolerant properties such as transversal gate implementation and modular gadget composition. Despite their conceptual appeal, these codes remain insufficiently characterized under operationally relevant conditions, specifically, under depth-limited recursion and realistic noise models where resource

efficiency is paramount.

Much of the existing QEC literature evaluates fault tolerance in asymptotic or idealized settings, offering limited insight into the performance of recursive, teleportation-based architectures under hardware-constrained conditions. In particular, there is a lack of simulation studies that incorporate both statistical rigor and architectural fidelity, especially across heterogeneous noise models and restricted recursion levels. This work addresses that gap by presenting a comprehensive simulation-based evaluation of the Fibonacci scheme, emphasizing empirical suppression behavior, resource-aware implementation, and benchmarking grounded in large-deviation theory.

### C. Novel Contribution of This Work

This study presents a comprehensive simulation-based analysis of the Fibonacci quantum error correction scheme under realistic hardware constraints. Departing from prior work focused on asymptotic thresholds or idealized recursion, we examine Level-1 and Level-2 encodings, targeting resource footprints compatible with current superconducting and trapped-ion platforms. Simulations are implemented using Qiskit’s stabilizer formalism, which efficiently models Clifford circuits while preserving key features of recursive teleportation.

To assess logical performance, we construct a statistically robust benchmarking framework that combines multi-level splitting, cross-entropy adaptive sampling, large-deviation theory, and Bayesian inference. This methodology enables high-resolution estimation of logical error rates across representative noise models, including Pauli channels, symmetric depolarizing noise, and mixed coherent errors. Importantly, the framework yields interpretable suppression metrics across both low- and moderate-noise regimes.

Results demonstrate consistent model-agnostic suppression, with approximately 50% reductions in logical error rates across all tested scenarios. We further estimate a fault tolerance threshold near 7

These findings position the Fibonacci architecture as a promising candidate for near-term fault-tolerant computing, particularly in settings constrained by coherence time, qubit connectivity, and ancilla availability. Its modular structure and selective recursion also suggest compatibility with hybrid QEC frameworks and compilation-level optimization strategies.

### D. Recursive Encoding Framework and Circuit Construction

The Fibonacci quantum error correction scheme employs logical teleportation as its core mechanism for fault-tolerant gate implementation and state transfer. Rather than serving solely as a communication primitive, teleportation is used to execute logical operations while confining fault propagation to localized subcircuits.

Originally proposed by Knill, the architecture extends postselection-based stabilizer schemes through recursive encoding with distance-2 codes, enhancing error detectability at each level. The structure is semi-concatenated: level- $J$  operations are constructed from fault-tolerant gadgets at

level  $J-1$ , enabling exponential suppression of logical errors under sub-threshold physical noise.

Logical operations are realized through modular subcircuits, or *gadgets*, each designed for tasks such as encoded CNOTs and logical measurements. Each gadget at level  $J$  is composed of independently verified level- $J-1$  components, maintaining recursive consistency and fault containment.

A defining feature of the scheme is the use of transversal gates, which apply operations in parallel across corresponding qubits in encoded blocks. For example, a logical CNOT is implemented via synchronized physical CNOTs between paired physical qubits. To limit error propagation, transversal gates are interleaved with teleportation layers that simultaneously extract error syndromes and implement logical transformations. This interleaving supports continuous error monitoring and restricts faults to confined regions of the circuit. [1][2]

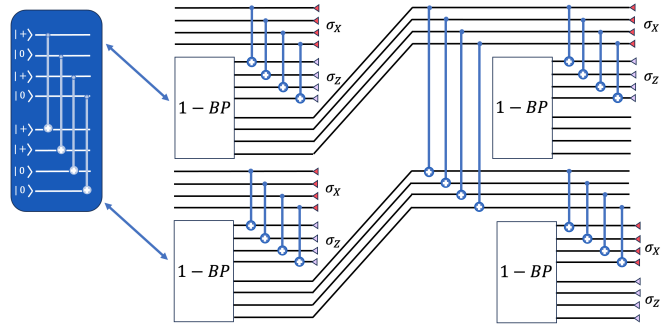


Figure 1 Fault-tolerant CNOT gadget protected by the C4 code. Transversal operations are interleaved with teleportation layers for syndrome extraction and fidelity preservation.

The architecture departs from full recursion in Bell pair preparation, which is implemented non-recursively to reduce entanglement overhead and circuit depth. This yields a hybrid structure, recursive in logical and correction layers, but flat in entanglement generation, striking a balance between fault tolerance and practical implementability.

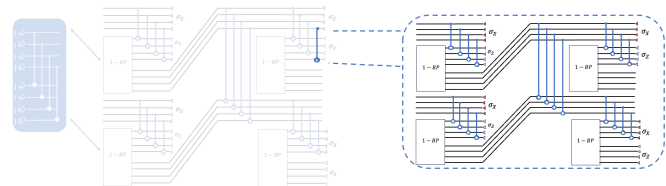


Figure 2 Semi-recursive structure: Logical operations at recursion level  $J$  are constructed from level- $J-1$  gadgets; Bell pair preparation remains non-recursive.

Simulations are performed in Qiskit using the stabilizer formalism, which efficiently supports classical emulation of Clifford circuits. Ancilla qubits are employed for entanglement mediation, syndrome extraction, and measurement decoding. Their modular integration across recursion levels facilitates gadget composability and compiler-level optimization.

While recursive encoding offers scalable suppression, circuit complexity increases exponentially with recursion

depth. Each additional level introduces substantial gate and qubit overhead, which is prohibitive under the constraints of NISQ devices. Accordingly, this work limits implementation to Level-1 and Level-2 recursion. Simulations confirm that even shallow recursion yields meaningful error suppression within available hardware budgets.

## E. Overview of the Paper

The remainder of this paper is organized as follows. Section **II** describes the construction and implementation of the Fibonacci quantum error correction scheme. Emphasis is placed on logical teleportation, selective recursion, and ancilla-assisted subcircuits as mechanisms for achieving fault tolerance under constrained hardware resources. Simulations are conducted within Qiskit’s stabilizer formalism to evaluate logical gate performance under representative noise models, including Pauli, depolarizing, and mixed coherent channels. Particular attention is given to CNOT gate error injection, reflecting its dominant contribution to overall circuit infidelity. Logical error characterization is supported by a multi-resolution statistical framework incorporating multi-level splitting, cross-entropy adaptive sampling, large-deviation analysis, and Bayesian inference.

Section **III** presents simulation results demonstrating consistent suppression of logical error rates across a range of physical noise strengths. The analysis reveals sublinear scaling behavior and identifies high-weight error pathways using large-deviation techniques. Bayesian inference enhances uncertainty quantification, while comparative benchmarks across recursion levels quantify the trade-offs between fault tolerance and resource demands. Results confirm that shallow recursion, specifically Level-1 and Level-2, yields meaningful suppression under near-term device constraints.

Section **IV** discusses the broader implications of this architecture. While deeper recursion increases implementation complexity, the scheme’s modular structure supports adaptive integration into hardware-aware QEC stacks. Potential extensions include hybridization with LDPC codes to reduce overhead further while maintaining fault isolation. Applications in quantum cryptography, molecular simulation, and combinatorial optimization are considered, where improved logical fidelity may yield direct algorithmic benefits. All simulation code and data are made available as open-source artifacts to support reproducibility and community benchmarking.

Together, these components offer a resource-conscious evaluation of recursive fault-tolerant quantum error correction, grounded in statistically rigorous simulation and attuned to practical deployment in NISQ-era hardware.

# II Methodology

## A. Simulation Model

Due to the substantial qubit and circuit-depth overhead intrinsic to the Fibonacci error correction scheme, direct hardware implementation on current quantum platforms remains infeasible. However, the scheme’s exclusive reliance on Clifford-group operations permits efficient classical simulation via the stabilizer formalism, enabling tractable bench-

marking of logical performance under realistic noise conditions.

Stabilizer circuits comprise operations from the Clifford group, including Hadamard ( $H$ ), Phase ( $S$ ), Pauli ( $X, Y, Z$ ), CNOT, and SWAP gates. These operations preserve stabilizer subspaces and are classically simulable under the Gottesman–Knill theorem, which asserts that quantum computations restricted to Clifford operations admit efficient polynomial-time simulation on classical hardware.

Formally, an  $n$ -qubit stabilizer state is defined by a set of  $n$  independent, commuting Pauli operators, known as stabilizer generators, whose joint +1 eigenspace specifies the encoded quantum state. Simulations track the evolution of this generator set under Clifford conjugation. While early stabilizer simulators incurred  $O(n^3)$  runtime complexity, recent advances leveraging symplectic representation and optimized data structures have reduced this to  $O(n^2)$ .

In this work, Qiskit’s stabilizer simulator is employed to evaluate the performance of the Fibonacci scheme under fault models representative of near-term quantum hardware. Noise is introduced through explicit injection at designated circuit locations, with emphasis on CNOT gates due to their dominant contribution to circuit-level infidelity in fault-tolerant architectures.[7][5]

Three representative noise models are considered:

- **Pauli channels:** Stochastic application of single-qubit Pauli errors ( $X, Y, Z$ ) with fixed probabilities.
- **Depolarizing noise:** Each qubit is replaced by a maximally mixed state with probability  $p$ , modeling uniform random error.
- **Mixed coherent noise:** A hybrid model combining stochastic Pauli errors with coherent over-rotation components, capturing both incoherent and unitary error dynamics.

This simulation framework offers multiple advantages: it supports scalable exploration of recursive code structures without requiring quantum hardware; enables fine-grained modeling of error propagation across circuit layers; and maintains full structural fidelity to the Fibonacci architecture. Accordingly, the stabilizer formalism provides a computationally efficient and architecturally faithful testbed for assessing logical error suppression and fault-tolerant behavior across experimentally relevant noise regimes.

## B. Noise Model

To evaluate the fault-tolerant performance of the Fibonacci error correction scheme under realistic operational conditions, we adopt a local stochastic noise model. A *location* is defined as any discrete instance of circuit execution, including qubit initialization, idle storage, gate operations, measurements, or classical feed-forward control. The model assumes uniform error susceptibility across all locations, providing an architecture-agnostic framework for assessing logical robustness.

Noise is introduced selectively at the gate level within the stabilizer simulation environment, with particular emphasis on CNOT gates, which are a dominant contributor to

circuit-level infidelity in Clifford-based architectures. Targeted perturbation of these operations enables controlled benchmarking of the scheme’s error suppression properties.

### B..1 Pauli Noise Model

The Pauli noise model provides a canonical abstraction for quantum error characterization. Errors are modeled as independent, stochastic applications of single-qubit Pauli operators:  $X$  (bit-flip),  $Z$  (phase-flip), and  $Y$  (bit-and-phase-flip), each occurring with probabilities  $p_X$ ,  $p_Z$ , and  $p_Y$ , respectively. Qubits are subject to these errors independently and identically distributed across circuit locations.

The action of each Pauli operator on a general state  $\alpha|0\rangle + \beta|1\rangle$  is given by:

$$X(\alpha|0\rangle + \beta|1\rangle) = \alpha|1\rangle + \beta|0\rangle, \quad (1)$$

$$Z(\alpha|0\rangle + \beta|1\rangle) = \alpha|0\rangle - \beta|1\rangle, \quad (2)$$

$$Y(\alpha|0\rangle + \beta|1\rangle) = -i\alpha|1\rangle + i\beta|0\rangle. \quad (3)$$

The resulting quantum operation for Pauli noise is described by:

$$\mathcal{N}(\rho) = (1-p)\rho + p_X X \rho X + p_Y Y \rho Y + p_Z Z \rho Z, \quad (4)$$

where  $p = p_X + p_Y + p_Z$  denotes the total error probability.

A common special case is the symmetric depolarizing channel, where  $p_X = p_Y = p_Z = p/3$ . This isotropic error model is widely adopted in fault-tolerant simulations for its simplicity and generality.

The Pauli noise model remains a standard in quantum error correction due to its analytical tractability under the stabilizer formalism and its compatibility with Clifford circuits. It provides a flexible and hardware-agnostic testbed for evaluating code performance across diverse platforms, including superconducting, trapped-ion, and photonic systems [6].

### B..2 Depolarizing Noise Model

The depolarizing noise model represents a symmetric limit of the general Pauli error framework, wherein all non-identity Pauli errors occur with equal probability. It serves as a canonical abstraction for unstructured noise and is widely adopted in fault-tolerance threshold studies due to its analytical simplicity and generality.

In this model, each qubit undergoes an independent Pauli error,  $X$ ,  $Y$ , or  $Z$ , with equal probability  $p/3$ , and remains unaffected with probability  $(1-p)$ . The single-qubit depolarizing channel is described by the quantum operation:

$$\mathcal{N}_{\text{depol}}(\rho) = (1-p)\rho + \frac{p}{3}(X\rho X + Y\rho Y + Z\rho Z). \quad (5)$$

The depolarizing channel imposes an isotropic error distribution, assigning equal weight to all Pauli components. This uniformity facilitates analytical derivations and efficient numerical simulations of logical error rates, making it a practical benchmark for assessing code performance under unbiased noise.

Crucially, the depolarizing channel preserves the stabilizer structure of quantum states, ensuring compatibility with Clifford-based simulation frameworks. This enables

large-scale evaluation of fault-tolerant protocols within the Gottesman–Knill formalism without compromising computational tractability.

In this study, the depolarizing model is employed as a baseline noise regime against which the error suppression capabilities of the Fibonacci scheme are quantitatively assessed.

### B..3 Dephasing Noise Model

The dephasing noise model characterizes environments where quantum coherence is predominantly degraded by phase-flip errors, a common decoherence mechanism in superconducting qubits and spin-based systems. In this model, only  $Z$ -type errors occur, reflecting a loss of phase information without affecting population probabilities.

The single-qubit dephasing channel is defined by the quantum operation:

$$\mathcal{N}_{\text{dephase}}(\rho) = (1-p_Z)\rho + p_Z Z \rho Z, \quad (6)$$

where  $p_Z$  denotes the probability of a phase-flip error.

This channel preserves the diagonal elements of the density matrix while attenuating off-diagonal coherence terms, modeling decoherence induced by low-frequency environmental fluctuations or quasi-static noise sources. Its structure captures the dynamics of phase randomization without population inversion, making it particularly relevant for hardware with dominant dephasing pathways.

The dephasing channel preserves Pauli symmetries and remains fully compatible with the stabilizer formalism, ensuring efficient simulation within Clifford-based circuit frameworks. This compatibility, combined with its empirical relevance, establishes dephasing noise as a standard benchmark for evaluating code performance under phase-dominated error regimes.

In this study, the dephasing model complements the depolarizing and Pauli noise channels, enabling a more granular assessment of the Fibonacci scheme’s fault-tolerance characteristics under system-specific decoherence profiles.

### B..4 Mixed Coherent Noise Model

To more faithfully represent quantum error dynamics, we incorporate a mixed coherent noise model that combines deterministic unitary errors with stochastic decoherence processes. This hybrid framework captures the dual character of noise observed in near-term quantum processors, where systematic control imperfections and random environmental interactions coexist.

The composite noise channel is defined as:

$$\mathcal{E}(\rho) = (1-p)U\rho U^\dagger + p\mathcal{N}(\rho), \quad (7)$$

where  $U$  represents unintended coherent evolution, arising from sources such as calibration drift or inter-qubit crosstalk, and  $\mathcal{N}(\rho)$  denotes a stochastic process, typically modeled via depolarizing or dephasing noise.

Coherent errors are modeled as unitary evolution under an undesired Hamiltonian  $H$ , with corresponding transformation:

$$U = \exp(-i\epsilon H), \quad (8)$$

where  $\epsilon$  quantifies the strength of deviation from the intended gate implementation.

To extend this framework, we define a weighted generalization that allows tunable contributions from both coherent and incoherent components:

$$\mathcal{E}_{\text{mixed}}(\rho) = (1 - \lambda) U \rho U^\dagger + \lambda [(1 - n)\rho + n \mathcal{N}(\rho)], \quad (9)$$

where  $\lambda \in [0, 1]$  specifies the stochastic noise weight, and  $n \in [0, 1]$  modulates the balance between identity preservation and incoherent degradation.

This composite model more accurately reflects operational error landscapes, offering a flexible benchmark for evaluating quantum error correction performance under diverse error regimes. By tuning the coherent-incoherent ratio, it becomes possible to probe code resilience across mixed-noise scenarios. Such modeling is particularly valuable in assessing schemes like the Fibonacci code, where recursive and teleportation-based architectures exhibit distinct sensitivity to coherent and incoherent fault propagation.

## C. Methodological Framework for Data Collection

### C..1 Notation and Formal Definitions

This subsection establishes a formal mathematical framework for characterizing data collection and performance evaluation within the Fibonacci quantum error correction scheme.

Let  $\mathcal{E}$  denote the space of possible physical error configurations encountered during code execution. Each element  $s \in \mathcal{E}$  represents a specific instantiation of qubit-level faults, including errors during initialization, idle storage, gate operations, or measurement processes.

Let  $\Theta$  denote the parameter space associated with the noise models under consideration. For a given parameter  $\theta \in \Theta$ , the corresponding noise process is defined by a probability distribution  $\mathcal{N}_\theta$  over  $\mathcal{E}$ . Error configurations are sampled according to:

$$s \sim \mathcal{N}_\theta(s). \quad (10)$$

As a concrete example, under a depolarizing noise model with error probability  $p \in [0, 1]$ , individual qubit errors are sampled independently from identical marginals. The joint distribution over  $n$  qubits is given by:

$$\mathcal{N}_p(e) = \prod_{q=1}^n \mathcal{N}_p(e_q), \quad (11)$$

where  $e_q$  denotes the error affecting the  $q$ -th qubit.

Let  $E \subseteq \mathcal{E}$  represent the set of error configurations that result in logical failure (e.g., uncorrectable errors or incorrect syndrome resolutions). The bit error rate (BER), denoted  $\text{BER}(\theta)$ , is defined as the probability measure of the failure set under  $\mathcal{N}_\theta$ :

$$\text{BER}(\theta) = \mathcal{N}_\theta(E). \quad (12)$$

For discrete configuration spaces, this reduces to:

$$\text{BER}(\theta) = \sum_{e \in E} \mathcal{N}_\theta(e), \quad (13)$$

while for continuous or hybrid spaces, the integral form applies:

$$\text{BER}(\theta) = \int_E \mathcal{N}_\theta(e) de. \quad (14)$$

These definitions provide a precise probabilistic foundation for subsequent estimation procedures and form the basis for quantitative evaluation of logical fault tolerance across parameterized noise regimes.

### C..2 Multi-Level Splitting

Accurate estimation of rare logical failure events in quantum error correction presents significant computational challenges, particularly at low physical error rates where conventional Monte Carlo sampling becomes intractable. To address this, we adopt the Multi-Level Splitting (MLS) technique, a stratified sampling method designed to improve efficiency in rare-event probability estimation.

Let  $E \subseteq \mathcal{E}$  denote the set of error configurations that result in logical failure. Under the noise model  $\mathcal{N}_\theta$ , the bit error rate (BER) corresponds to the total probability mass assigned to  $E$ :

$$\text{BER}(\theta) = \sum_{s \in E} \mathcal{N}_\theta(s), \quad (15)$$

or in integral form for continuous or hybrid spaces:

$$\text{BER}(\theta) = \int_E \mathcal{N}_\theta(s) ds. \quad (16)$$

In the MLS framework, the configuration space  $\mathcal{E}$  is partitioned into a nested sequence of subsets:

$$\mathcal{E}_0 \subset \mathcal{E}_1 \subset \dots \subset \mathcal{E}_L = \mathcal{E}, \quad (17)$$

where each level  $\mathcal{E}_\ell$  consists of configurations satisfying a predefined complexity constraint. A common stratification strategy defines levels by error weight:

$$\mathcal{E}_\ell = \{e \in \mathcal{E} \mid \text{weight}(e) \leq \ell\}, \quad (18)$$

where  $\text{weight}(e)$  denotes the number of affected qubits in configuration  $e$ . Lower levels capture high-probability, low-weight errors, while upper levels include increasingly rare configurations contributing to logical failure.

The total failure probability is decomposed into a product of conditional transition probabilities:

$$\mathcal{N}_\theta(E) = \prod_{\ell=1}^L \mathcal{N}_\theta(\mathcal{E}_\ell \mid \mathcal{E}_{\ell-1}), \quad (19)$$

with each term defined as:

$$\mathcal{N}_\theta(\mathcal{E}_\ell \mid \mathcal{E}_{\ell-1}) = \frac{\mathcal{N}_\theta(\mathcal{E}_\ell)}{\mathcal{N}_\theta(\mathcal{E}_{\ell-1})}. \quad (20)$$

By estimating each conditional transition independently, MLS reduces the global estimation problem into a sequence of tractable subproblems confined to progressively higher-weight regions of the error space. This hierarchical decomposition enables concentrated sampling in failure-relevant regions, improving statistical efficiency without incurring the exponential cost of full enumeration.

MLS thus provides a robust and scalable methodology for quantifying rare logical failure events. Its ability to resolve low-probability tails with high fidelity renders it especially effective for benchmarking fault-tolerant QEC architectures across diverse noise regimes.

### C..3 Cross-Entropy Optimization for Importance Sampling

To enhance rare-event estimation efficiency beyond what is achieved by Multi-Level Splitting (MLS) alone, we incorporate the Cross-Entropy (CE) method, a statistical optimization framework originally developed within inference theory for adaptive importance sampling. Unlike cross-entropy benchmarking techniques used in quantum gate fidelity estimation, the present formulation is applied to iteratively refine the sampling distribution during Monte Carlo evaluation of logical error rates [3].

Within the MLS hierarchy, CE serves as a mechanism for adapting the sampling distribution at each intermediate level  $\mathcal{E}_\ell$ . The objective is to concentrate sampling on configurations with elevated likelihood of contributing to logical failure, thereby improving the efficiency of estimating the bit error rate (BER).

At each level  $\ell$ , samples are initially drawn from a parameterized importance distribution  $Q_{\ell-1}(\alpha_{\ell-1})$ , which serves as a proxy for the physical noise model  $\mathcal{N}_\theta$ . Among these samples, an elite subset  $S_\ell^{\text{elite}}$  is selected based on a performance criterion, such as the conditional transition probability from  $\mathcal{E}_{\ell-1}$  to  $\mathcal{E}_\ell$ . This elite set identifies configurations most indicative of failure-inducing behavior at the current level.

A new parametric family of distributions  $Q_\ell(\alpha_\ell)$  is then introduced to refine sampling at level  $\ell$ . The optimal parameter vector  $\alpha_\ell^*$  is obtained by maximizing the likelihood of the elite set under  $Q_\ell(\alpha_\ell)$ :

$$\alpha_\ell^* = \arg \max_{\alpha_\ell} \sum_{e \in S_\ell^{\text{elite}}} \log Q_\ell(\alpha_\ell; e). \quad (21)$$

Equivalently, this optimization minimizes the Kullback–Leibler (KL) divergence between the empirical distribution of elite samples and the parametric family  $Q_\ell(\alpha_\ell)$ , aligning subsequent sampling with high-impact regions of the error space.

This process produces a sequence of progressively refined importance distributions:

$$Q_0(\alpha_0) \rightarrow Q_1(\alpha_1) \rightarrow \dots \rightarrow Q_L(\alpha_L^*), \quad (22)$$

each tuned to its respective level's critical error subset.

The CE method offers two primary advantages. First, it reduces estimator variance by adaptively reallocating sampling effort toward failure-dominant configurations, thereby increasing the statistical reliability of BER estimates. Second, its flexible parametric representation accommodates a broad range of system-specific noise structures, including correlated or non-uniform error models.

Together with MLS, CE provides a scalable and principled mechanism for distributional control in rare-event simulation. This hybrid strategy enables high-resolution, computationally efficient benchmarking of fault-tolerant quantum error correction codes across diverse operational regimes. [3]

### C..4 Bayesian Updating and Uncertainty Quantification

Bayesian inference provides a coherent statistical framework for quantifying uncertainty in performance metrics such as

the bit error rate (BER). Let  $\psi$  denote a latent parameter representing the underlying logical failure probability, and let  $\pi(\psi)$  denote a prior distribution encoding initial uncertainty before empirical observation.

Following a finite number of simulation trials, during which  $D$  logical failures are recorded, the posterior distribution is derived via Bayes' theorem:

$$\pi(\psi | D) \propto \pi(\psi) \cdot L(D | \psi), \quad (23)$$

where  $L(D | \psi)$  is the likelihood function, quantifying the probability of observing  $D$  failures given  $\psi$ .

The resulting posterior distribution  $\pi(\psi | D)$  captures the updated probabilistic characterization of  $\psi$  after incorporating empirical data. From this distribution, point estimates such as the posterior mean, mode, or median represent central tendency measures, while the posterior variance quantifies estimation uncertainty. Posterior credible intervals further provide probabilistically grounded uncertainty bounds, offering an alternative to frequentist confidence intervals.

This inferential framework confers several methodological advantages. First, it explicitly accounts for sampling variability, producing robust estimates under small-sample conditions and rare-event regimes. Second, Bayesian updating supports sequential inference: the posterior from one dataset naturally serves as a prior for subsequent trials, enabling adaptive simulation strategies. Third, posterior distributions allow comparative analysis across heterogeneous noise models and system configurations, supporting performance benchmarking under varying physical regimes.

In the context of quantum error correction, Bayesian methods enable rigorous uncertainty quantification in BER estimation, identification of high-variance regions in the error landscape, and principled guidance for sample allocation and code parameter tuning. As such, Bayesian inference constitutes a core component of statistically disciplined evaluation pipelines for fault-tolerant quantum architectures.

### C..5 Large Deviation Analysis and Logarithmic Performance Metrics

Large Deviation Analysis (LDA) provides a complementary framework to Multi-Level Splitting (MLS) and Cross-Entropy (CE) sampling by characterizing the asymptotic behavior of tail distributions associated with rare, high-weight error configurations. Although these events occur with low probability, they often dominate the statistical profile of logical failure, particularly in low-noise regimes.

In this context, the error configuration space  $\mathcal{E}$  is stratified by syndrome complexity and decoder response, enabling analytical isolation of extreme-event trajectories that deviate significantly from mean error behavior. By capturing these rare-event dynamics, LDA quantifies the statistical weight of high-impact error pathways beyond what is accessible through naïve sampling.

Operationally, LDA is implemented in conjunction with CE-based importance sampling, which directs sampling density toward the tail regions identified as high-contribution zones. This integration improves estimation precision in low-noise regimes, where uniform sampling becomes statistically inefficient. Moreover, insights from LDA can guide

the construction of MLS stratification thresholds, enhancing adaptivity across heterogeneous noise landscapes.

To standardize performance evaluation and enable cross-scheme comparison, the bit error rate (BER) is expressed in logarithmic form:

$$-\log(\text{BER}), \quad (24)$$

which linearizes exponential differences in logical error probability and compresses the dynamic range for interpretable benchmarking.

Representative values include:

- $-\log(\text{BER}) = 1$ :  $\text{BER} = 10^{-1}$ , indicating minimal error suppression.
- $-\log(\text{BER}) = 5$ :  $\text{BER} = 10^{-5}$ , consistent with near-term quantum hardware performance targets.
- $-\log(\text{BER}) = 10$ :  $\text{BER} = 10^{-10}$ , reflecting thresholds required for scalable fault-tolerant architectures.

This logarithmic formulation provides a hardware-agnostic abstraction layer, allowing code performance to be evaluated independently of specific physical architectures or noise parameterizations. In practice, values of  $-\log(\text{BER}) > 5$  are generally considered indicative of feasibility for noisy intermediate-scale quantum (NISQ) systems, while values approaching or exceeding 10 signal the robustness expected in fully fault-tolerant regimes.

Together, LDA and logarithmic performance metrics form an integrated diagnostic framework. While LDA quantifies the statistical contributions of extreme error pathways, the  $-\log(\text{BER})$  scale provides a concise, interpretable metric for cross-code benchmarking. This combination offers a rigorous foundation for evaluating the efficacy of the Fibonacci error correction scheme under realistic operational conditions.

## C..6 Convergence Diagnostics and Posterior Reliability

In Bayesian inference for quantum error correction benchmarking, convergence diagnostics are essential to ensure the validity and interpretability of posterior distributions derived from Markov Chain Monte Carlo (MCMC) sampling. Accurate characterization of these distributions underpins performance estimation and credible uncertainty quantification.

A standard diagnostic is the Gelman–Rubin statistic, denoted  $\hat{R}$ , which compares within-chain and between-chain variance across independently initialized MCMC runs. Formally,

$$\hat{R} \approx 1 \Rightarrow \text{Satisfactory convergence.} \quad (25)$$

Values of  $\hat{R}$  approaching unity indicate that chains have mixed well and that the sampled distribution reliably represents the target posterior. In contrast, elevated  $\hat{R}$  values reflect poor convergence and may lead to biased estimates or mischaracterized credible intervals.

Once convergence is verified, posterior distributions yield both central estimates (e.g., posterior mean or median) and credible intervals that define probabilistic bounds for performance metrics such as the bit error rate (BER). These

intervals provide a coherent quantification of epistemic uncertainty and are particularly informative in sparse-event regimes, where point estimates alone may be misleading.

Credible intervals support several key objectives. First, they quantify statistical confidence associated with fault-tolerance thresholds across varying noise models. Second, they facilitate rigorous comparison between code configurations, highlighting trade-offs between resource overhead and performance stability. Third, they inform adaptive design by identifying parameter regimes with elevated uncertainty, where additional sampling or code refinement is warranted.

In this framework, convergence diagnostics and posterior reliability are not ancillary components but integral elements of a statistically principled evaluation methodology. Their inclusion ensures that inference-based conclusions regarding quantum error correction schemes are both robust and reproducible, supporting high-confidence benchmarking and informed architectural decisions in fault-tolerant quantum system design.

## C..7 Summary of Methodological Framework

The proposed methodological framework establishes a scalable and statistically principled approach for evaluating the performance of the Fibonacci quantum error correction scheme under hardware-relevant noise conditions. By integrating Multi-Level Splitting (MLS), Cross-Entropy (CE) adaptive sampling, Bayesian inference, and stabilizer-based simulation, the framework achieves a calibrated balance between computational tractability, model generality, and inferential rigor.

A central contribution of this framework is the hierarchical decomposition of the error configuration space, enabling stratified sampling of failure-inducing configurations across heterogeneous noise models, including Pauli, depolarizing, dephasing, and mixed coherent channels. This decomposition facilitates systematic exploration of the error landscape and supports the identification of dominant failure mechanisms under varying operational regimes.

The adaptive refinement of sampling distributions via CE optimization further enhances computational efficiency by concentrating effort on statistically consequential regions of configuration space. This targeted allocation improves the resolution of bit error rate (BER) estimates, particularly in low-noise regimes where rare-event dynamics dominate performance outcomes.

Bayesian inference complements the sampling architecture by providing robust uncertainty quantification. Posterior distributions yield credible intervals and performance bounds, supporting rigorous interpretation of logical error suppression even under sparse-sample conditions. Expressing BER in logarithmic form,  $-\log(\text{BER})$ , standardizes performance metrics, enabling cross-code comparison and improving interpretability across architectures and noise regimes.

The overall framework offers both analytical generality and practical adaptability. It is well-suited for benchmarking fault-tolerant code performance in both simulation environments and near-term experimental platforms. The full implementation, including stabilizer circuit construction, noise injection protocols, and statistical evaluation routines, is publicly available at: <https://github.com/EricKim1942/Fibonacci-Meets->

Quantum-Computing <https://github.com/EricKim1942/Fibonacci> Meets-Quantum-Computing, supporting reproducibility and collaborative advancement in quantum error correction research. [4]

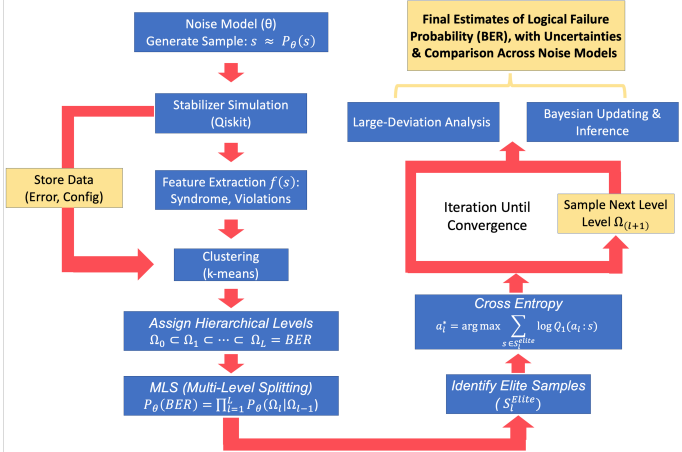


Figure 3 Large deviation analysis of depolarizing noise in the Fibonacci error correction scheme under the stabilizer formalism.

#### D. Practical QPU Alignment: Hardware Considerations for Fibonacci QEC Implementation

While the Fibonacci error correction scheme demonstrates robust performance in simulation, practical deployment on quantum processing units (QPUs) necessitates alignment with hardware-specific constraints. Effective implementation requires not only logical error suppression but also architectural compatibility with superconducting, trapped-ion, and photonic qubit platforms.

Superconducting QPUs, such as IBM's Falcon and Eagle architectures, offer rapid gate execution but are limited by two-dimensional nearest-neighbor connectivity. As a result, the non-local transversal operations intrinsic to recursive stabilizer codes incur routing overhead via SWAP insertion, increasing circuit depth and susceptibility to decoherence. Logical teleportation in the Fibonacci scheme partially mitigates this by localizing gate execution and constraining fault propagation. However, fidelity loss in entangled Bell pairs and ancillary qubit overhead remain limiting factors. Given current coherence times and gate fidelities, recursion beyond Level-2 is generally infeasible on superconducting platforms.

Trapped-ion systems, exemplified by IonQ's architectures, provide all-to-all connectivity and extended coherence times, supporting deeper recursion and higher-fidelity logical operations. These platforms are particularly well-suited to teleportation-based schemes due to reliable entanglement distribution. Nonetheless, slower gate speeds and limited ancilla availability impose practical constraints, typically restricting implementations to Level-2 recursion with careful ancilla scheduling and Bell pair circuit optimization.

Photonic processors, such as those developed by Xanadu and PsiQuantum, offer modularity and high-fidelity entanglement generation but lack native two-qubit gate primitives, complicating stabilizer code execution. Despite this, the modular and teleportation-centric architecture of the Fi-

bacci scheme is conceptually compatible with photonic platforms. In practice, the depth of stabilizer circuits and the complexity of multi-qubit operations constrain recursion to Level-1 under current hardware limitations.

Overall, the recursive and teleportation-based structure of the Fibonacci scheme affords a degree of architectural flexibility not available in surface code frameworks. However, optimal integration necessitates calibration of recursion depth against platform-specific constraints in connectivity, gate fidelity, and qubit availability. Near-term deployment is most feasible using shallow recursion (Level-1 or Level-2), balanced against hardware trade-offs.

Future directions include hybrid QEC architectures embedding Fibonacci modules within surface or low-density parity-check (LDPC) codes, as well as compiler-level optimizations that map recursive circuits onto device-specific connectivity graphs. Such strategies will be critical in enhancing the practical viability of Fibonacci QEC in scalable, fault-tolerant quantum computing environments.

## III Results

### A. Low-Noise Regime

To assess the baseline performance of the Fibonacci error correction scheme, simulations were conducted under low physical noise conditions, with error probabilities ranging from  $10^{-5}$  to  $10^{-2}$ . This interval was discretized into 500 logarithmically uniform steps, with each configuration evaluated via 50,000 Monte Carlo trials to ensure statistical convergence.

As an initial diagnostic, a canonical bit-flip (Pauli-X) noise model was employed to isolate the scheme's intrinsic suppression capabilities under uncorrelated stochastic errors.

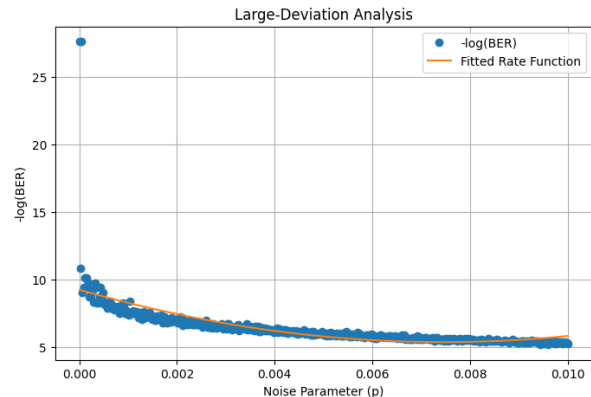


Figure 4 Large deviation analysis under bit-flip noise using the Fibonacci code within the stabilizer formalism.

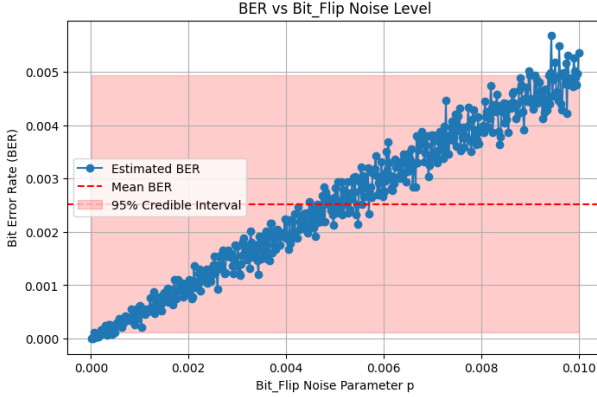


Figure 5 Bit error rate (BER) under bit-flip noise in the Fibonacci code at low physical error probabilities.

To evaluate resilience against hardware-relevant error behavior, simulations were extended to a mixed coherent noise model incorporating both stochastic Pauli errors and systematic unitary over-rotations. This composite channel better reflects practical deviations from idealized depolarizing noise.

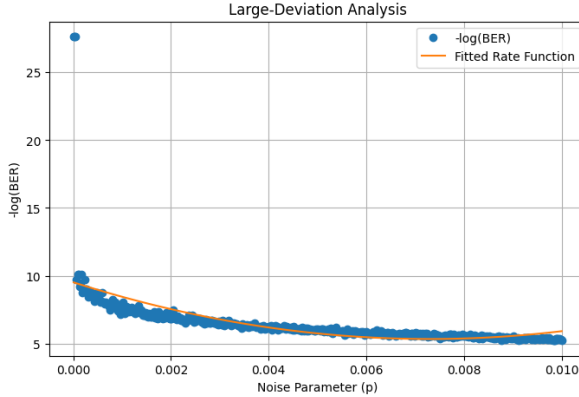


Figure 6 Large deviation analysis under mixed coherent noise at low noise levels.

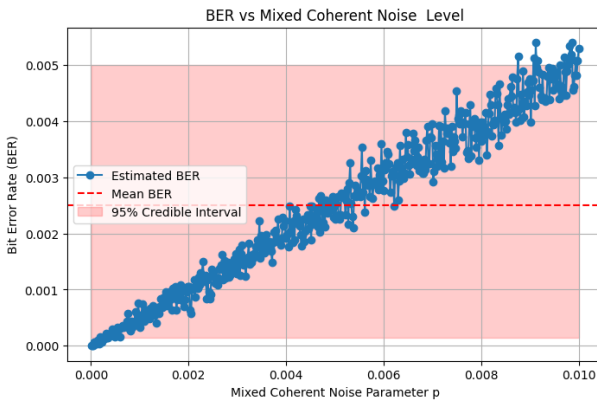


Figure 7 BER under mixed coherent noise in the Fibonacci code.

Across both noise models, the BER exhibits consistent exponential suppression in the low-noise regime, as evidenced by linear trends in  $-\log(\text{BER})$ . This behavior aligns

with theoretical expectations for recursively encoded stabilizer codes, where hierarchical encoding restricts high-weight error propagation.

The scheme maintains robust performance across Pauli, depolarizing, and coherent channels, highlighting its model-agnostic suppression characteristics and architectural generality. Minor deviations at ultra-low error rates are attributed to statistical variance and decoder threshold effects, reflecting rare, high-weight fault trajectories that merit further decoder optimization.

Preliminary slope comparisons indicate improved suppression with increased recursion depth, although at the cost of resource overhead. Formal scaling analysis could help quantify this trade-off under physical hardware constraints.

## B. Moderate–High Noise Regime

To assess the performance limits of the Fibonacci scheme under adverse conditions, simulations were extended to moderate-to-high physical noise levels ( $p = 0.01$  to  $0.5$ ). These regimes test the resilience of first-level recursion schemes in domains where fault tolerance is typically challenged.

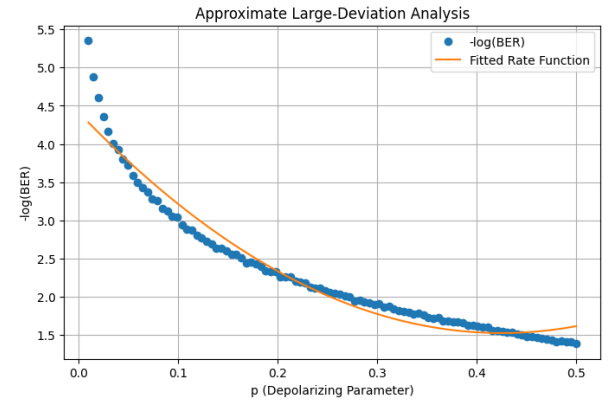


Figure 8 Large deviation analysis under depolarizing noise. Best-fit model:  $-\log(\text{BER}) \approx 4.415 - 13.59p + 15.98p^2$ .

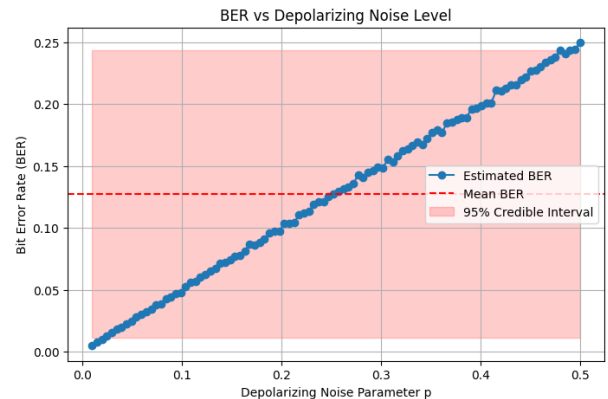


Figure 9 BER under depolarizing noise in the Fibonacci code at moderate-to-high physical error rates.

Despite uniformly distributed error channels, the Fibonacci scheme exhibits sublinear BER growth, underscoring its continued suppression efficacy under recursive encoding.

For comparative benchmarking, bit-flip noise simulations were performed under equivalent conditions.

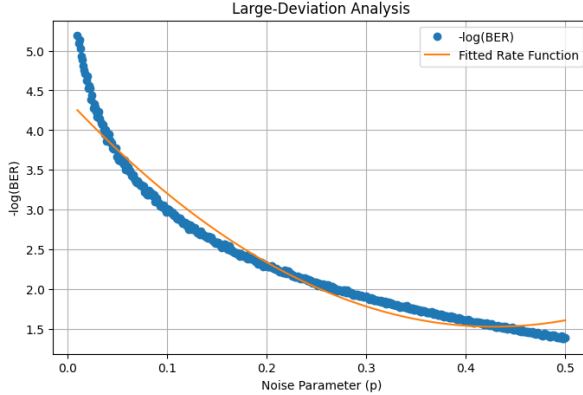


Figure 10 Large deviation analysis under bit-flip noise. Best-fit model:  $-\log(\text{BER}) \approx 4.384 - 13.336p + 15.574p^2$ .

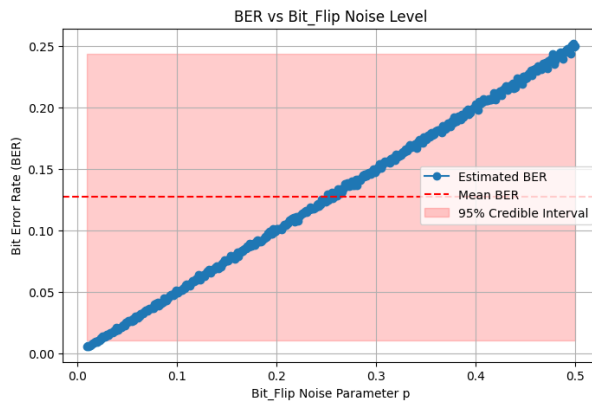


Figure 11 BER under bit-flip noise at moderate-to-high error probabilities.

Mixed coherent noise simulations further highlight the scheme’s fault-tolerance under structured unitary-stochastic composite channels.

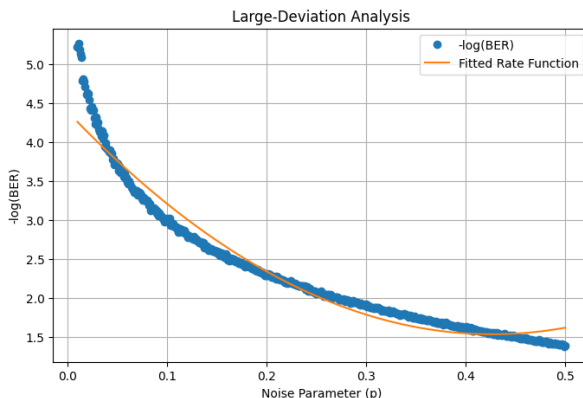


Figure 12 Large deviation analysis under mixed coherent noise. Best-fit model:  $-\log(\text{BER}) \approx 4.391 - 13.408p + 15.71p^2$ .

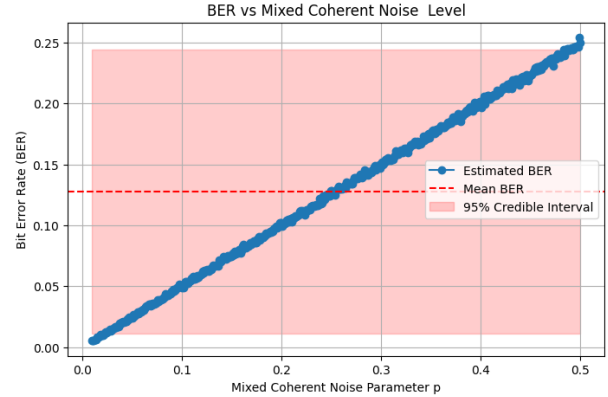


Figure 13 BER under mixed coherent noise in the Fibonacci code.

Across all regimes, the Fibonacci code demonstrates reliable suppression behavior. In the  $p < 0.3$  range, BER scaling closely matches theoretical predictions, while values above this threshold exhibit sublinear degradation, indicative of residual fault confinement. Notably, even under extreme error conditions, suppression does not fully collapse, reflecting the inherent robustness of recursive code structure.

Large Deviation Analysis (LDA) further dissects failure modes by identifying high-weight error configurations contributing disproportionately to logical failure. These events, underrepresented in uniform sampling, are efficiently isolated through LDA-based stratification. Transition zones in the tail distribution mark regions where decoder capacity is increasingly strained, yet not exceeded.

Clustering analysis applied within the LDA framework reveals structurally recurring fault patterns, providing actionable diagnostic insight into potential decoder refinements or the design of auxiliary correction layers.

Together, BER and LDA metrics offer complementary perspectives: while BER quantifies macroscopic logical fidelity, LDA characterizes microscopic error pathways. This dual-analysis framework supports comprehensive performance assessment under diverse noise models.

The consistent scaling behavior across Pauli, depolarizing, and coherent channels underscores the code’s model-agnostic resilience. Even in resource-constrained recursion regimes, the Fibonacci scheme delivers competitive suppression relative to conventional codes.

These findings validate the scheme’s viability for near-term fault-tolerant deployment and highlight the utility of advanced statistical diagnostics, particularly LDA and logarithmic BER scaling, as general-purpose benchmarking tools for quantum error correction architectures.

### C. Threshold Calculation

The fault-tolerance threshold of the Fibonacci error correction scheme can be analytically estimated by modeling the recursive suppression of logical error rates across successive encoding levels. Let  $P_{L,k}$  denote the logical error probability at recursion level  $k$ , and let  $p$  represent the baseline physical error rate. The recursive update for  $P_{L,k}$  is modeled as:

$$P_{L,k+1} = c \cdot P_{L,k}^2 + b \cdot p \cdot P_{L,k}, \quad (26)$$

where  $c$  quantifies the contribution from higher-order error terms, and  $b$  captures the first-order propagation of physical noise through the encoded circuit.

At threshold, the system reaches a steady state such that  $P_{L,k+1} = P_{L,k} = P_L$ . Substituting this fixed-point condition yields:

$$P_L = c \cdot P_L^2 + b \cdot p_c \cdot P_L. \quad (27)$$

Assuming  $P_L > 0$ , dividing both sides by  $P_L$  gives:

$$1 = c \cdot P_L + b \cdot p_c. \quad (28)$$

In the asymptotic limit  $P_L \rightarrow 0$ , the threshold simplifies to:

$$p_c = \frac{1}{b}. \quad (29)$$

To estimate  $b$ , we utilize empirical fits from Large Deviation Analysis (LDA). The scaling function  $S(p)$ , which describes the behavior of  $-\log(\text{BER})$  under varying physical error rates, is modeled as:

$$S(p) = 4.39 + 13.4p + 15.7p^2. \quad (30)$$

The local sensitivity of logical failure rates to  $p$  is approximated by the derivative:

$$b(p) = \frac{dS(p)}{dp} = 13.4 + 2 \cdot 15.7p. \quad (31)$$

At low noise rates, the linear term dominates, yielding  $b \approx 13.4$ .

Additionally, simulations indicate a near-linear empirical relationship between BER and  $p$ , approximated as:

$$\text{BER} \approx r \cdot p, \quad \text{with } r \approx 0.45. \quad (32)$$

This relation implies a consistent suppression factor across recursion levels, and can be incorporated into the fixed-point model to refine the threshold expression:

$$p_c = \frac{1 - c}{r \cdot b}. \quad (33)$$

Assuming  $c \approx 0.45$  and using the previously estimated  $b = 13.4 + 2 \cdot 15.7p_c$ , we obtain the self-consistent equation:

$$p_c = \frac{0.55}{0.45 \cdot (13.4 + 31.4p_c)}. \quad (34)$$

Multiplying both sides yields the quadratic form:

$$15.7p_c^2 + 6.7p_c - 0.55 = 0. \quad (35)$$

Solving via the quadratic formula:

$$p_c = \frac{-6.7 \pm \sqrt{6.7^2 + 4 \cdot 15.7 \cdot 0.55}}{2 \cdot 15.7}. \quad (36)$$

Evaluating the discriminant:

$$\sqrt{44.89 + 34.54} = \sqrt{79.43} \approx 8.91. \quad (37)$$

Thus, the positive root yields:

$$p_c \approx \frac{-6.7 + 8.91}{31.4} \approx \frac{2.21}{31.4} \approx 0.0704 \text{ (or 7.0%).} \quad (38)$$

This result suggests that, under the assumption of consistent first-order suppression and sublinear error propagation, the Fibonacci scheme remains effective for physical error rates below approximately 7%. Operating above this threshold necessitates either deeper recursion or enhanced decoder optimization to maintain fault-tolerant behavior.

## D. Comparison with Other Quantum Error Correction Codes

Code	Noise Types	Threshold	BER Scaling	Overhead	Key Insights and Comparison
Shor's Code	Bit-Flip/ Phase Flip	<10%	Exponential degradation	High	Benchmark for early QECCs; impractical for modern devices.
LDPC Codes	Depolarizing	0.5%-1%	Consistent	Low (if dense qubit connectivity)	Efficient error suppression with scalable overhead for hardware with good connectivity
Steane Code	Pauli (Bit-Flip/ Phase Flip)	<0.01%	Rapid degradation at high noise	Moderate	Effective at low noise; scales poorly above p>0.01
Surface Code	Depolarizing	1%-2%	Sublinear for p<0.1	High (planar lattice stabilizers)	Strong threshold; well-suited for large-scale systems but high qubit cost.
Bacon-Shor Code	Mixed Coherent/ Asymmetric	<5%	Degrades for symmetric noise	Low	Strong for asymmetric noise but weaker for uniform noise
Fibonacci QECC	Pauli, Depolarizing, Mixed Coherent	5% - 10%	Consistently reduces noise by 50%	Extremely High (due to recursion depth)	Robust across noise types; uniquely effective in consistently halving noise regardless of intensity.

Figure 14 Comparative analysis of quantum error correction codes based on threshold performance and noise model adaptability.

The Fibonacci quantum error correction code (QECC) exhibits a distinct operational profile relative to conventional architectures such as surface codes, Steane codes, Shor's code, and low-density parity-check (LDPC) codes. Its principal advantage lies in its consistent logical error suppression across heterogeneous noise models, including Pauli, depolarizing, and mixed coherent channels. This model-agnostic performance distinguishes it from many alternatives that are typically optimized for specific error regimes (e.g., surface codes for depolarizing noise, LDPC codes for structured connectivity environments).

Empirical analysis demonstrates that the Fibonacci scheme achieves an approximate 50% reduction in logical error rates across a broad spectrum of physical noise parameters. This suppression remains comparatively invariant to noise composition, in contrast to other codes whose performance deteriorates outside their optimal operating envelopes. For instance, Shor's code, while offering a relatively high theoretical threshold (approaching 10%), suffers from substantial overhead and lacks modular scalability. Steane codes, though compatible with transversal gate constructions, exhibit a considerably lower practical threshold (often below 0.01%), limiting their applicability in noisy intermediate-scale quantum (NISQ) settings.

Threshold analysis indicates that the Fibonacci code remains operationally viable at physical error rates up to approximately 5%-10%, outperforming surface codes (typically 1%-2%) and offering more robust suppression under moderate noise levels. While LDPC codes provide low-overhead implementations and favorable decoding complexity, their performance is often constrained by hardware-specific connectivity assumptions and decoding latency factors not uniformly supported across near-term platforms.

The primary trade-off in the Fibonacci scheme is its recursive encoding structure, which introduces nontrivial overhead in qubit count and circuit depth. However, its modular composition, enabled by teleportation layers and partial recursion, facilitates architectural flexibility. In contrast to the spatial lattice constraints of surface codes or the rigid layering of fully concatenated schemes, the Fibonacci framework allows tunable recursion depth and component-level modularity, enabling more tailored integration with device-level constraints.

In summary, the Fibonacci QECC broadens the design landscape for fault-tolerant architectures by offering a tunable, architecture-agnostic encoding strategy with broad noise compatibility and recursive modularity. While overhead considerations require calibrated deployment strategies, its consistent suppression behavior and structural adaptability make it a strong candidate for hybrid code compositions, compiler-optimized mapping routines, and distributed quantum computing frameworks.

## IV Discussion

### A. Key Observations and Performance Summary

The Fibonacci quantum error correction (QEC) scheme exhibits consistent logical error suppression across a broad spectrum of noise environments, including Pauli, depolarizing, and mixed coherent channels. Simulations demonstrate an approximate 50% reduction in logical error rates, independent of specific physical error models, a suppression profile aligned with theoretical predictions for recursively concatenated stabilizer codes. These results underscore the scheme's relevance for near-term quantum devices operating below fault-tolerance thresholds.

Central to this performance is the recursive encoding structure, which enables hierarchical error mitigation. Lower recursion levels suppress localized low-weight faults, while higher levels extend protection to more complex error configurations. Although the present implementation is constrained to two recursion layers due to resource limitations, observed trends suggest that deeper concatenation could further enhance logical fidelity, provided qubit counts, coherence times, and connectivity improve.

Fault-tolerant operation is supported by transversal gate implementations and teleportation-based logical operations. These mechanisms effectively localize error propagation and facilitate scalable circuit construction, particularly in distributed architectures such as superconducting, trapped-ion, and photonic systems. Logical teleportation enables inter-module communication without physical qubit transport, thereby reducing cumulative decoherence risk in hardware-constrained platforms.

The implementation, developed within Qiskit's stabilizer framework, provides a reproducible and extensible testbed for benchmarking under realistic noise models. The exclusive use of Clifford-group operations permits efficient classical simulation, while the modular circuit design ensures compatibility with broader QEC paradigms.

Nevertheless, recursive encoding imposes nontrivial resource overhead. Each additional level increases both qubit

count and circuit depth exponentially, and ancillary qubits required for Bell pair generation, syndrome extraction, and measurement decoding exacerbate these demands. Such scaling challenges are particularly limiting in the NISQ regime.

Addressing these constraints may involve hybrid architectures, where Fibonacci layers are combined with low-density parity-check (LDPC) codes or other sparse encodings. In such configurations, LDPC layers can efficiently correct low-weight errors, while Fibonacci recursion handles high-weight fault isolation, balancing overhead and performance. Complementary strategies include advanced decoders (e.g., belief propagation for LDPC sublayers) and hardware-aware code parameterization tailored to platform-specific gate sets, connectivity graphs, and noise profiles.

Beyond error suppression, the scheme's recursive modularity positions it as a flexible component in quantum algorithm pipelines. Applications in quantum chemistry, variational optimization, cryptography, and quantum machine learning stand to benefit from improved logical fidelity, enhancing algorithmic convergence and runtime stability.

Moreover, the open-source release supports community-driven development and educational integration. The structured architecture not only enables comparative benchmarking but also provides a didactic platform for curriculum development in quantum computing pedagogy.

Finally, the scheme introduces a structured framework for performance characterization. Metrics such as fidelity-to-overhead ratios, logical error suppression per recursion level, and decoder latency offer actionable benchmarks for code selection in heterogeneous architectures. These attributes collectively position the Fibonacci QEC scheme as a scalable and architecture-agnostic solution within fault-tolerant quantum computing ecosystems.

### B. Cross-Disciplinary Analogies and Conceptual Interpretations

The recursive structure of the Fibonacci quantum error correction code exhibits conceptual parallels with renormalization group (RG) transformations in statistical physics. In both frameworks, successive layers integrate local fluctuations into coarser effective descriptions. Higher recursion levels in the Fibonacci scheme progressively suppress lower-weight error modes, mirroring the coarse-graining of short-range correlations along RG flow. This analogy offers an interpretive lens for understanding the emergence of fault-tolerance thresholds and the scaling behavior of logical error suppression.

The hierarchical encoding also reflects a form of self-similarity analogous to fractal compression in classical information theory. In such schemes, recursive redundancy enables scalable information protection while preserving structural economy. Viewed through this lens, the Fibonacci code may be interpreted as a fractalized redundancy protocol, wherein the recursive structure balances suppression efficacy with encoding overhead. This perspective introduces an alternative framework for analyzing redundancy efficiency and saturation effects in logical error propagation as recursion depth increases.

Further conceptual correspondence arises in the layered

transmission of syndromes across the decoding hierarchy, which resembles distributed optimization in network coding theory. Structured redundancy in network systems enables data recovery over lossy communication channels; analogously, the Fibonacci decoder aggregates syndrome information across recursive layers to reconstruct logical states. This similarity suggests potential decoder design pathways informed by flow networks and graph-theoretic error propagation models.

These analogies extend beyond illustrative value. They provide formal insight into the structural organization and dynamical behavior of fault-tolerant quantum codes. By situating the Fibonacci scheme within broader theoretical frameworks from statistical physics, information theory, and distributed systems, these interpretations may inform novel encoding strategies, hierarchical decoders, and resource-aware design principles in next-generation quantum error correction.

### C. Limitations and Future Directions

While the Fibonacci quantum error correction scheme demonstrates consistent logical error suppression across diverse noise models, several limitations remain that warrant further investigation.

First, the current implementation is restricted to two levels of recursion, limiting the ability to probe the scheme’s asymptotic performance. Although theoretical models predict exponential suppression with increasing recursion depth, practical deployment remains constrained by physical qubit availability, circuit depth, and coherence times. Future work should explore scalable simulation techniques or hardware-efficient approximations to assess higher-level concatenation under realistic conditions.

Second, the simulations assume idealized syndrome extraction and perfect measurement fidelity, omitting readout errors that constitute a significant failure mode in experimental QPUs. Moreover, noise injection is localized to CNOT gates, neglecting error contributions from state preparation, single-qubit rotations, measurement operations, and temporally correlated (non-Markovian) noise factors known to influence performance in real-world architectures. Extending the noise model to encompass these channels would yield a more comprehensive assessment of scheme robustness.

Third, the decoding architecture remains static and non-adaptive. It lacks mechanisms to dynamically adjust to syndrome structure, evolving error statistics, or fluctuations in the underlying noise profile. Incorporating adaptive decoding strategies, potentially inspired by belief propagation, reinforcement learning, or network-theoretic inference, could enhance decoder fidelity under heterogeneous operational regimes.

Finally, the framework does not yet incorporate a formal cost-performance model to quantify trade-offs between logical fidelity, qubit overhead, and circuit complexity across platforms. Developing such a model would support systematic code optimization and facilitate architecture-aware deployment strategies.

Addressing these limitations opens several directions for future research. Enhancing the simulation environment to

include measurement noise, correlated error processes, and temporally structured faults would improve diagnostic granularity. Benchmarking the scheme across multiple hardware backends would enable platform-specific performance profiling. Additionally, hybrid QEC architectures, combining Fibonacci recursion with low-density parity-check (LDPC) pre-encoding layers, could reduce resource overhead while preserving high logical fidelity. Such layered constructions may offer a more favorable balance between suppression efficacy and implementation cost, particularly in hardware-constrained regimes.

More broadly, integrating decoder adaptivity, architectural cost modeling, and cross-platform benchmarking will be essential for realizing the full potential of the Fibonacci scheme within scalable fault-tolerant quantum computing frameworks.

### D. Theoretical Extensions and Research Outlook

This work opens several theoretical directions that merit further exploration. One critical area is the development of a formal scaling law that quantifies the relationship between recursion depth and fault-tolerance thresholds. A generalization of the Aliferis–Preskill framework may provide closed-form expressions for logical error rates as a function of concatenation level and noise model parameters, enabling more predictive assessments of code performance.

A second avenue involves the design of adaptive decoding strategies. Syndrome-space clustering could be used to enhance decoder resolution and reduce computational complexity by identifying dominant error patterns. The integration of machine learning techniques may further refine decision boundaries in high-dimensional syndrome spaces and dynamically adapt decoding policies to evolving noise environments.

Hybrid architectures that combine recursive stabilizer codes with low-overhead error-filtering layers, such as low-density parity-check codes or repetition codes, present an opportunity for developing analytical models of composite fidelity-to-overhead tradeoffs. Such models could guide resource allocation strategies in platform-constrained settings, optimizing code structure in accordance with hardware capabilities.

Another important direction involves analyzing the behavior of the Fibonacci scheme under temporally correlated and spatially structured noise. Understanding the code’s stability under non-Markovian dynamics could reveal structural vulnerabilities and inform modifications that enhance robustness in practical implementations.

As quantum processors continue to scale toward intermediate-size architectures, addressing these theoretical dimensions will be essential to enabling fault-tolerant quantum computing beyond the current capabilities of noisy intermediate-scale quantum (NISQ) devices.

## References

- [1] Panos Aliferis, Daniel Gottesman, and John Preskill. “Quantum accuracy threshold for concatenated

- distance-3 codes”. In: *arXiv preprint quant-ph/0504218* (2005).
- [2] Panos Aliferis and John Preskill. “Fibonacci scheme for fault-tolerant quantum computation”. In: *Physical Review A—Atomic, Molecular, and Optical Physics* 79.1 (2009), p. 012332.
- [3] Pieter-Tjerk de Boer. *A Tutorial on the Cross-Entropy Method*. [https://web.mit.edu/6.454/www/www-fall\\_2003/gew/CEtutorial.pdf](https://web.mit.edu/6.454/www/www-fall_2003/gew/CEtutorial.pdf). [Accessed 02-01-2025]. 2003.
- [4] JA Bravo-Montes et al. “A methodology to select and adjust quantum noise models through emulators: benchmarking against real backends”. In: *EPJ Quantum Technology* 11.1 (2024), p. 71.
- [5] Peter Brooks and John Preskill. “Fault-tolerant quantum computation with asymmetric Bacon-Shor codes”. In: *Physical Review A—Atomic, Molecular, and Optical Physics* 87.3 (2013), p. 032310.
- [6] Daniel Gottesman. “Surviving as a Quantum Computer in a Classical World. 2024”. In: URL <https://www.cs.umd.edu/class/spring2024/cmse858G/QECCbook-2024-ch1-11.pdf> (2024).
- [7] C Ryan-Anderson et al. “High-fidelity teleportation of a logical qubit using transversal gates and lattice surgery”. In: *Science* 385.6715 (2024), pp. 1327–1331.